

Supporting information for:

**Isocyanate Deinsertion from κ^1 -O Amides: Facile Access
to Perfluoroaryl Rhodium(I) Complexes**

Marcus W. Drover, Laurel L. Schafer,* and Jennifer A. Love*

Department of Chemistry, The University of British Columbia, 2036 Main Mall,
Vancouver, British Columbia, Canada V6T 1Z1

1. Spectral data for Rh(I) amide complexes	S-2
2. Crystallographic data tables	S-19

Figure S1. 2. ^1H NMR, C_6D_6 , 600 MHz, 298K

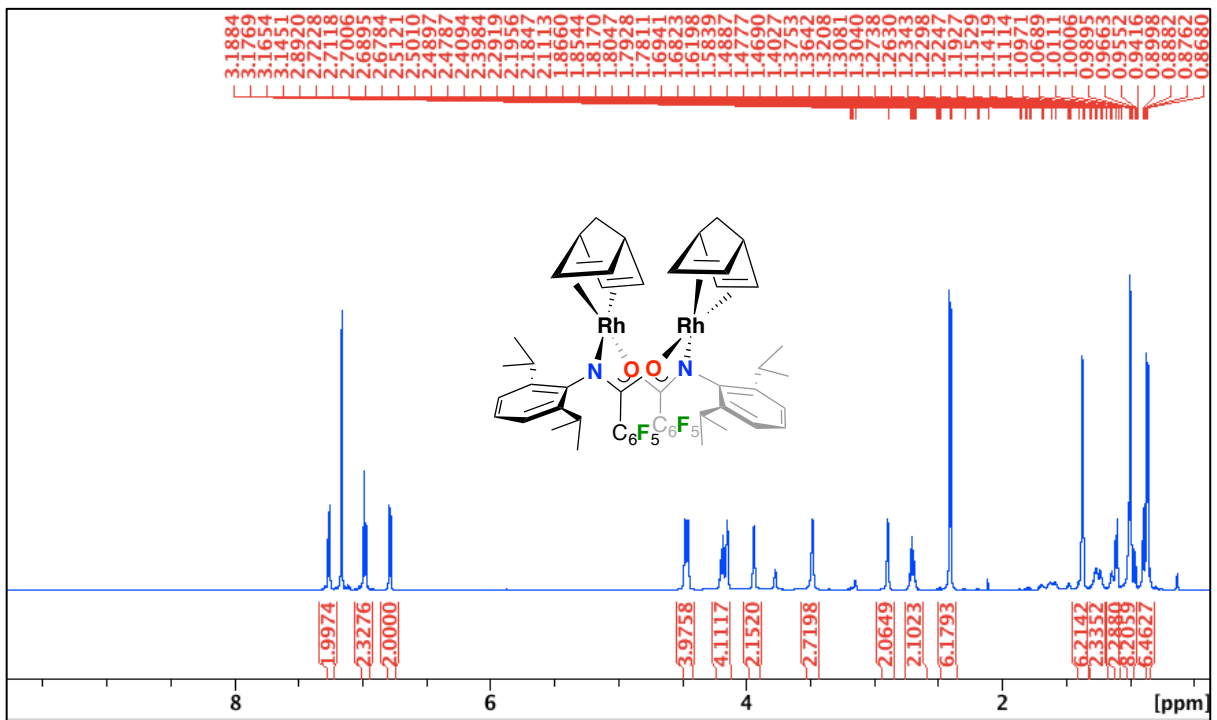


Figure S2. 2. $^{19}\text{F}\{^1\text{H}\}$ NMR, C_6D_6 , 377 MHz, 298 K

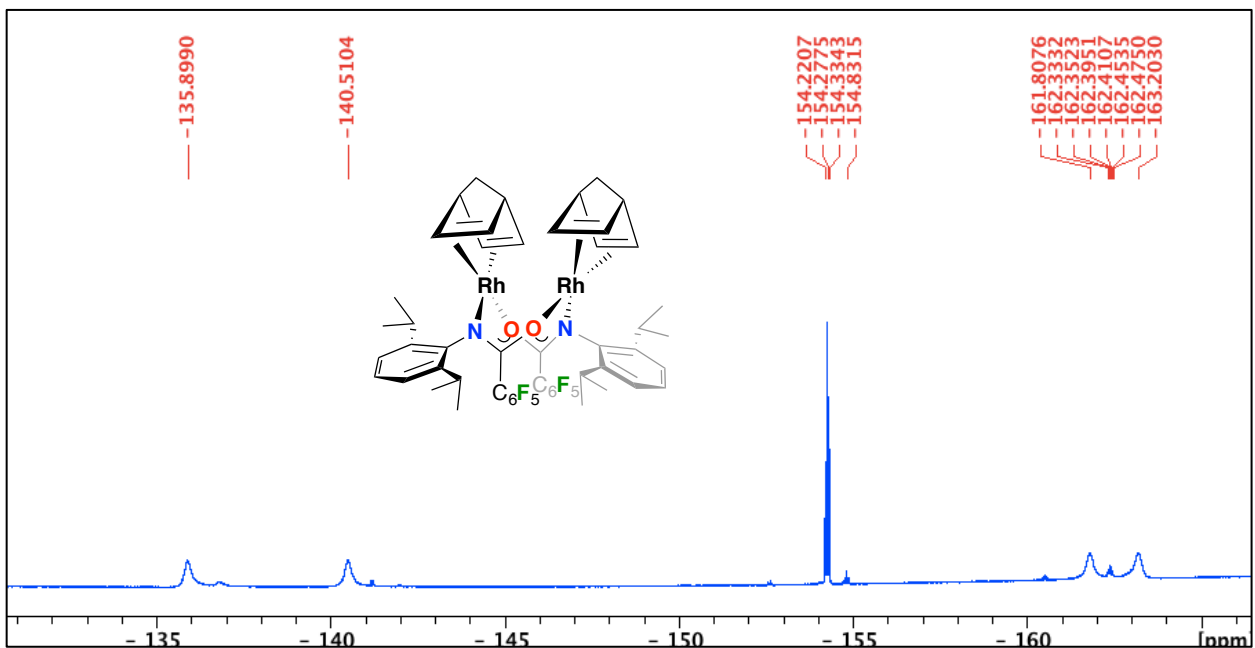


Figure S3. 2, $^{13}\text{C}\{\text{H}\}$ NMR, C_6D_6 , 150 MHz, 298 K

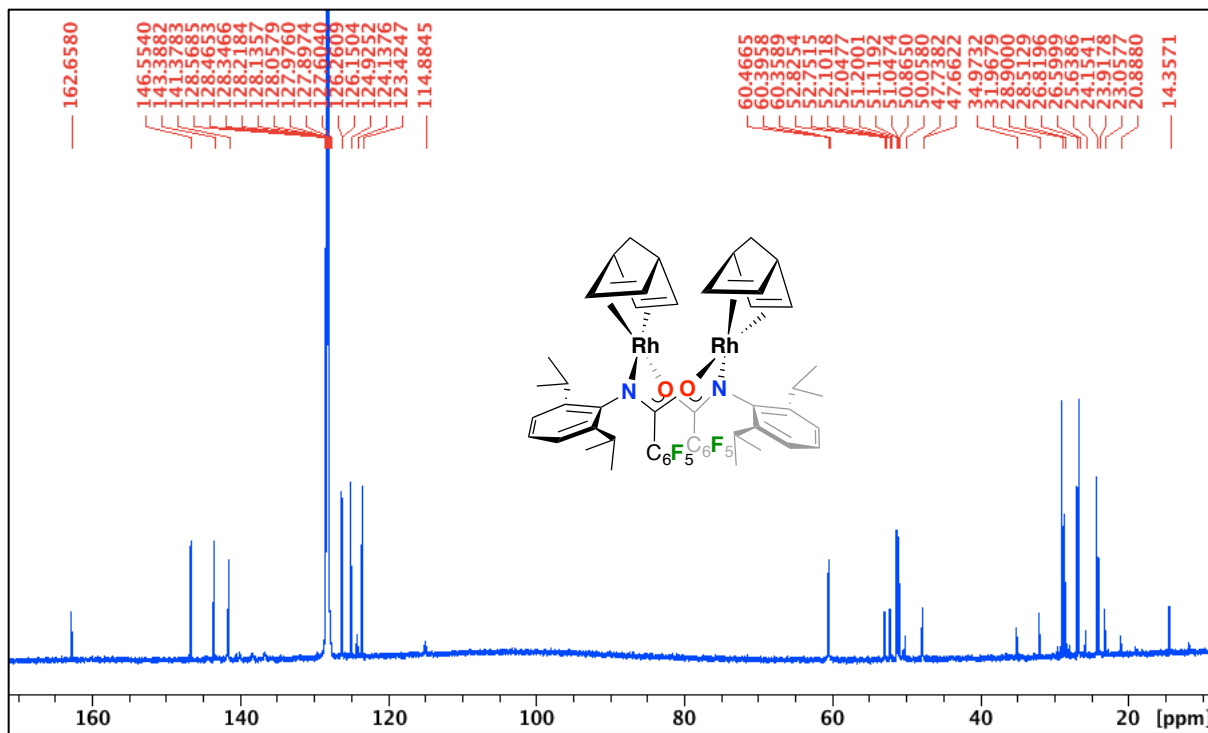


Figure S4. E/Z-3, ^1H NMR, tol- d_8 , 300 MHz, 298 K

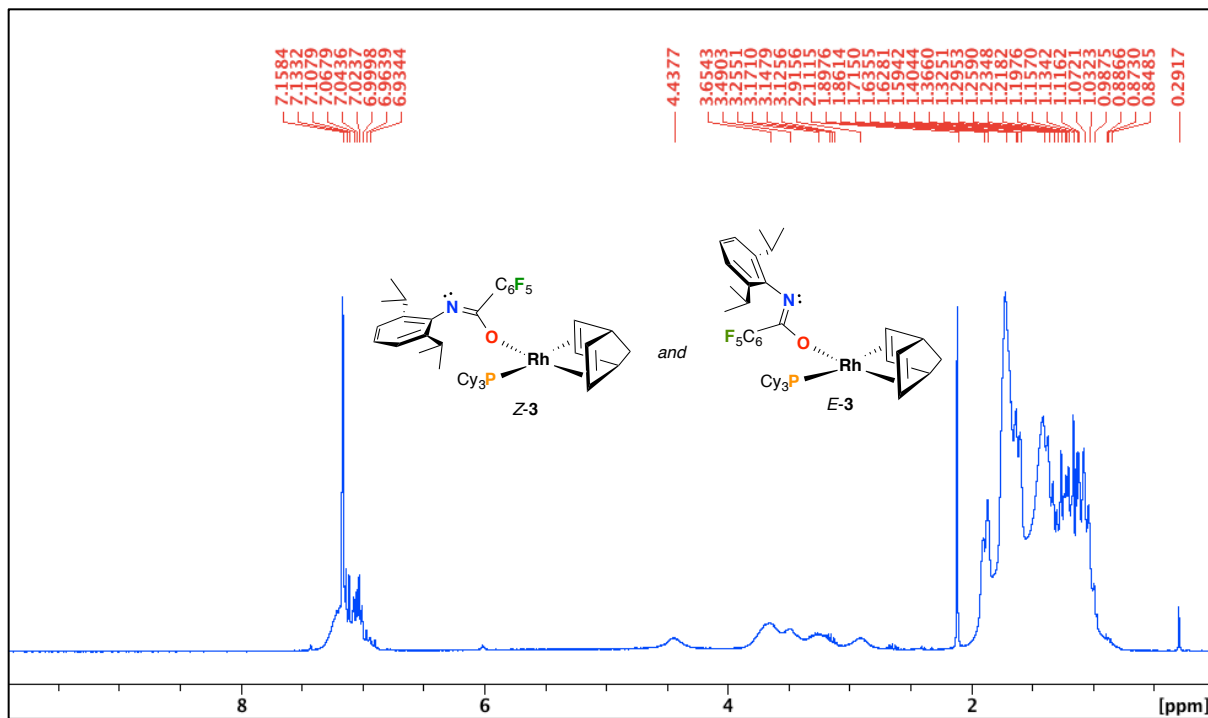


Figure S5. *E/Z-3*, VT ^1H NMR, tol- d_8 , 300 MHz (* = residual $\text{Rh}(\eta^4\text{-NBD})(\text{PCy}_3)\text{Cl})$

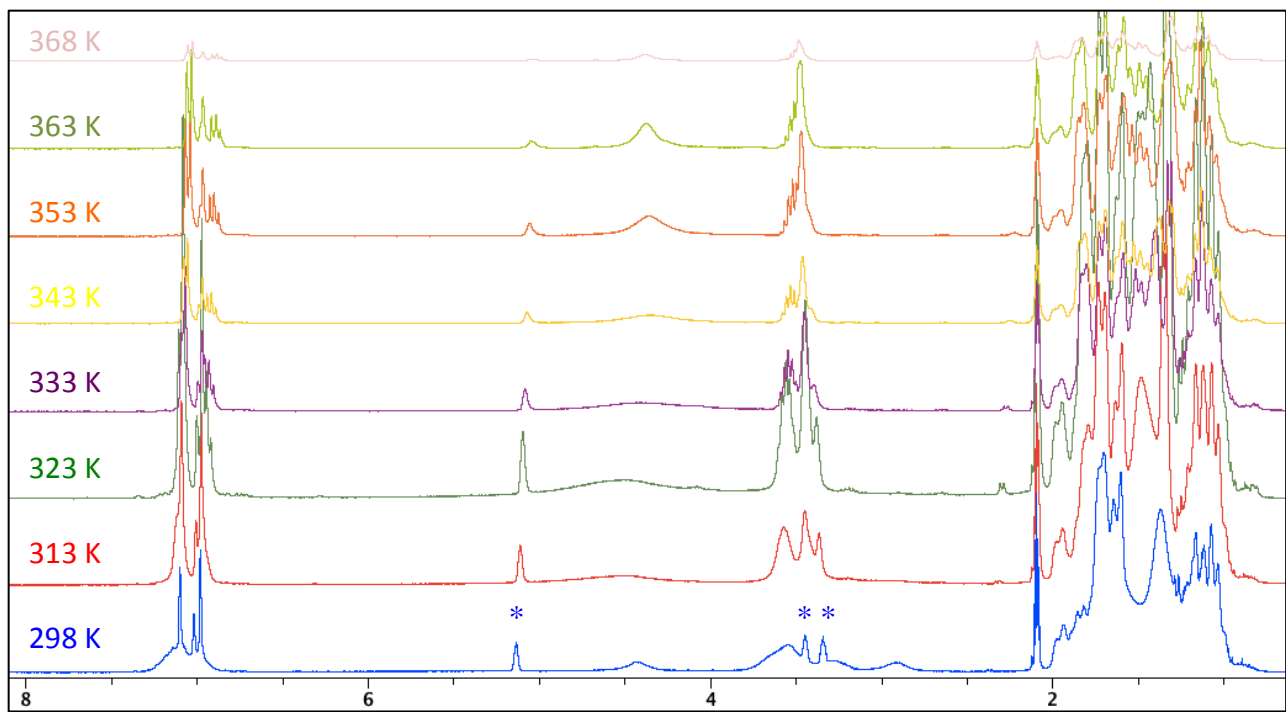


Figure S6. *E/Z-3*, $^{31}\text{P}\{\text{H}\}$ NMR, tol- d_8 , C₆D₆, 121 MHz, 298 K

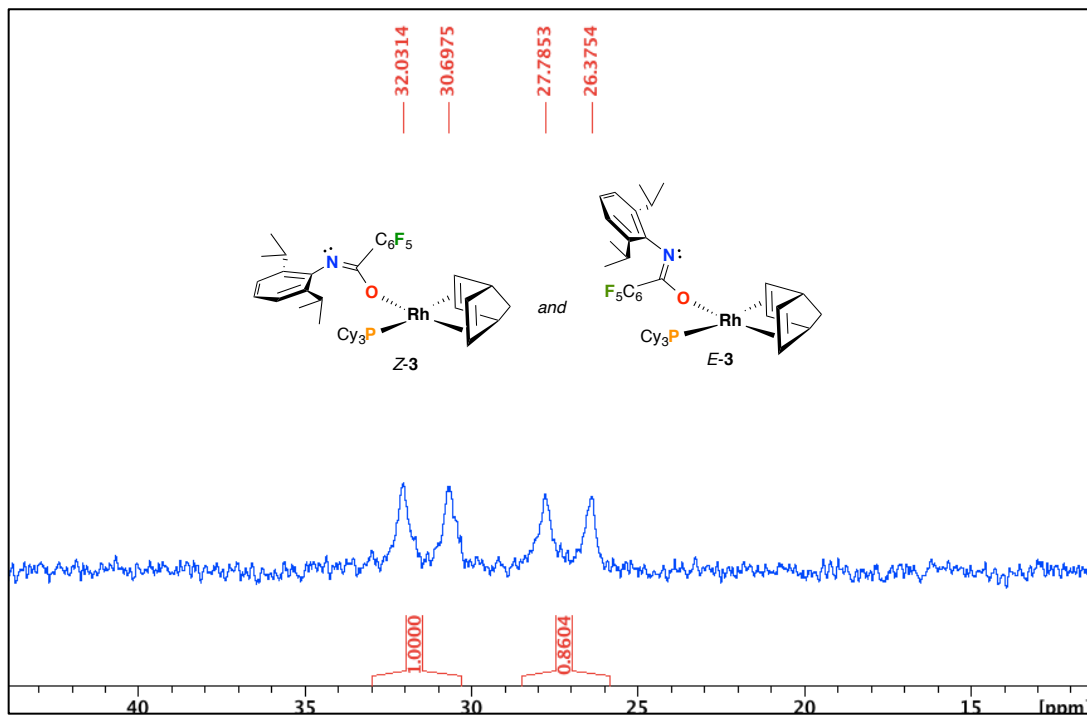


Figure S7. *E/Z-3*, VT $^{19}\text{F}\{^1\text{H}\}$ NMR, tol- d_8 , 282 MHz

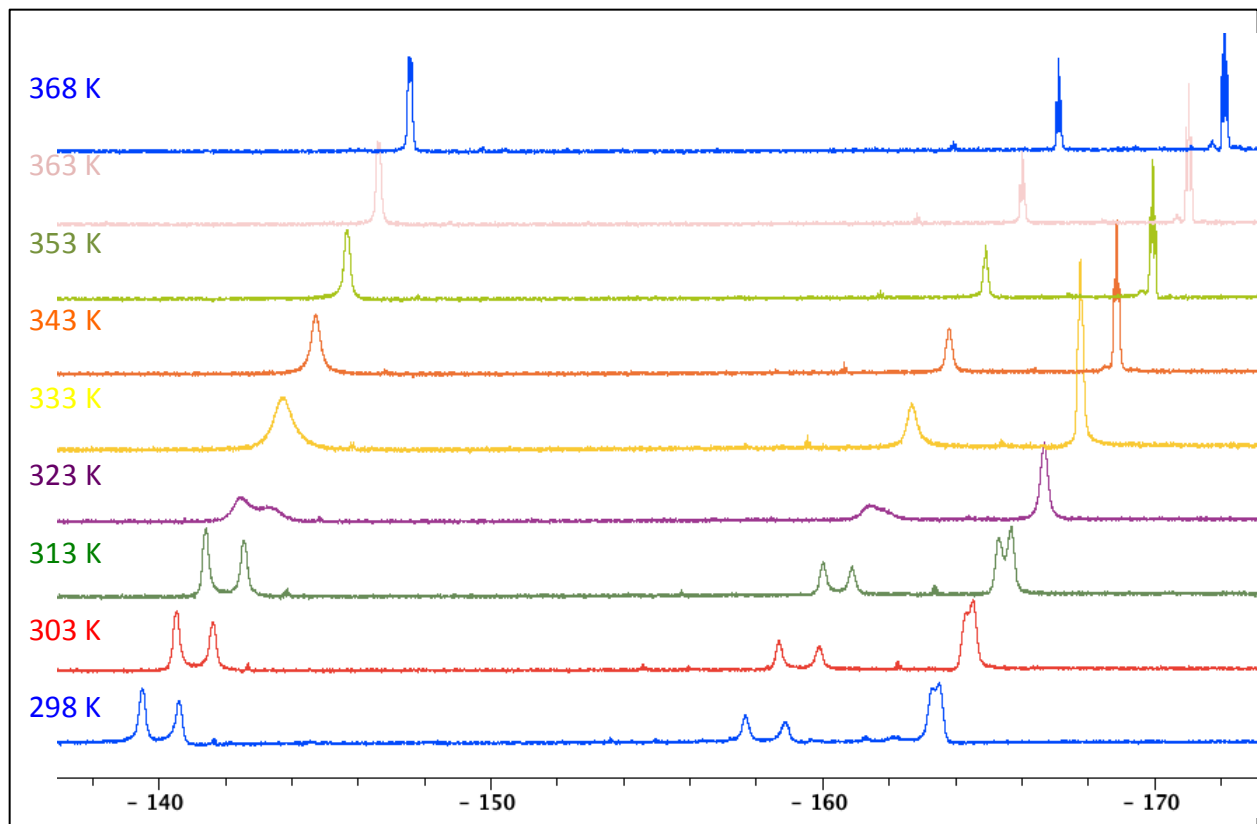


Figure S8. *E/Z-3*, solid-state IR (ATR) spectrum, 298 K

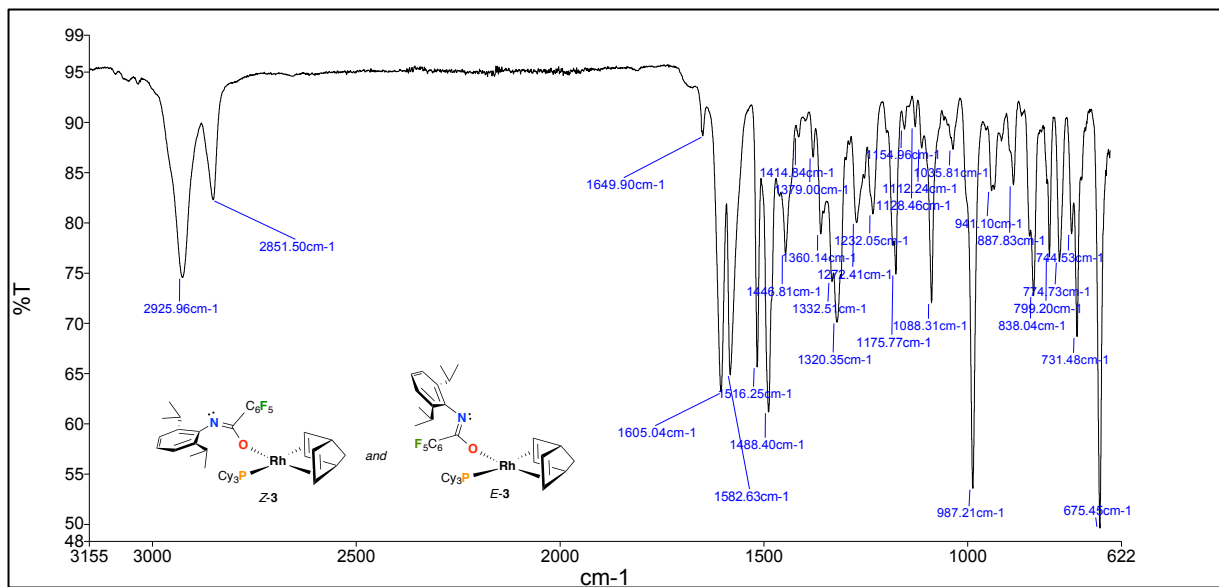


Figure S9. **5**, ^1H NMR, C_6D_6 , 400 MHz, 298K

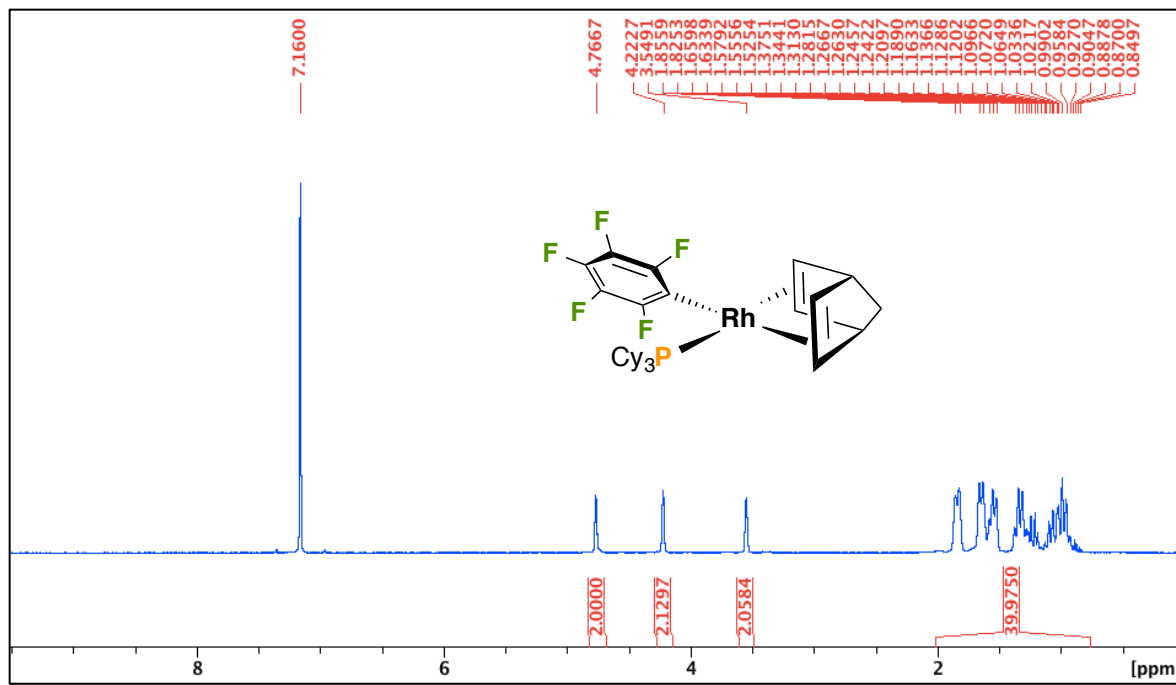


Figure S10. **5**, $^{19}\text{F}\{^1\text{H}\}$ NMR, C_6D_6 , 377 MHz, 298 K

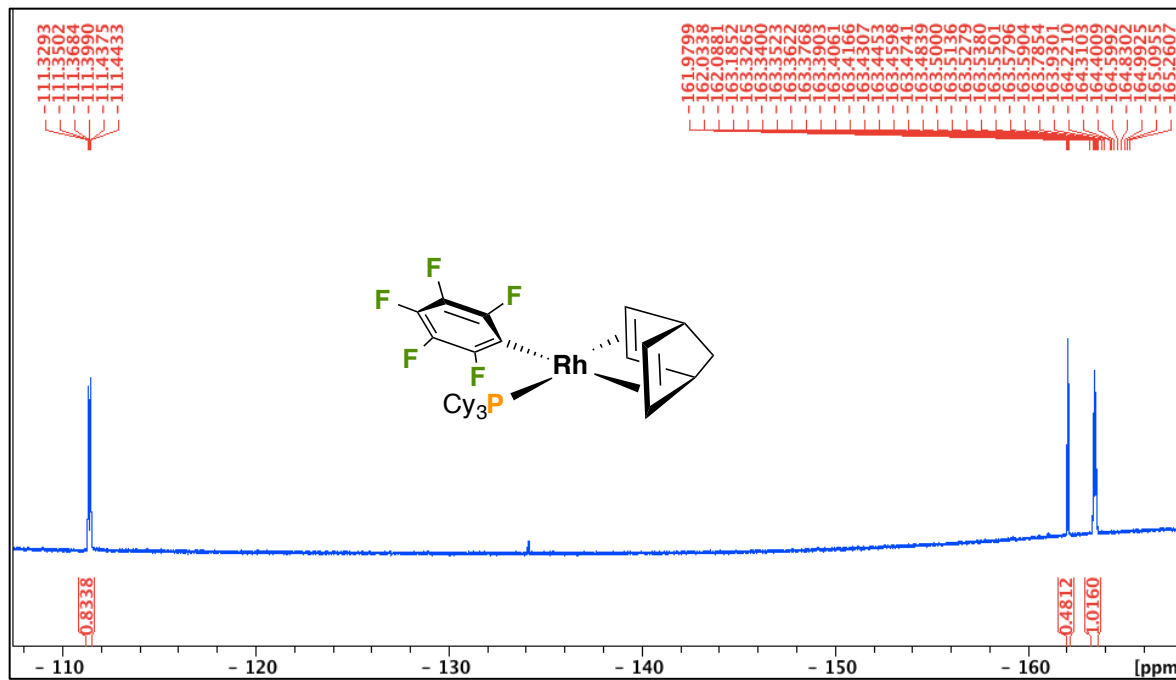


Figure S11. ${}^5\text{S}$, ${}^{31}\text{P}\{{}^1\text{H}\}$ NMR, C_6D_6 , 162 MHz, 298 K

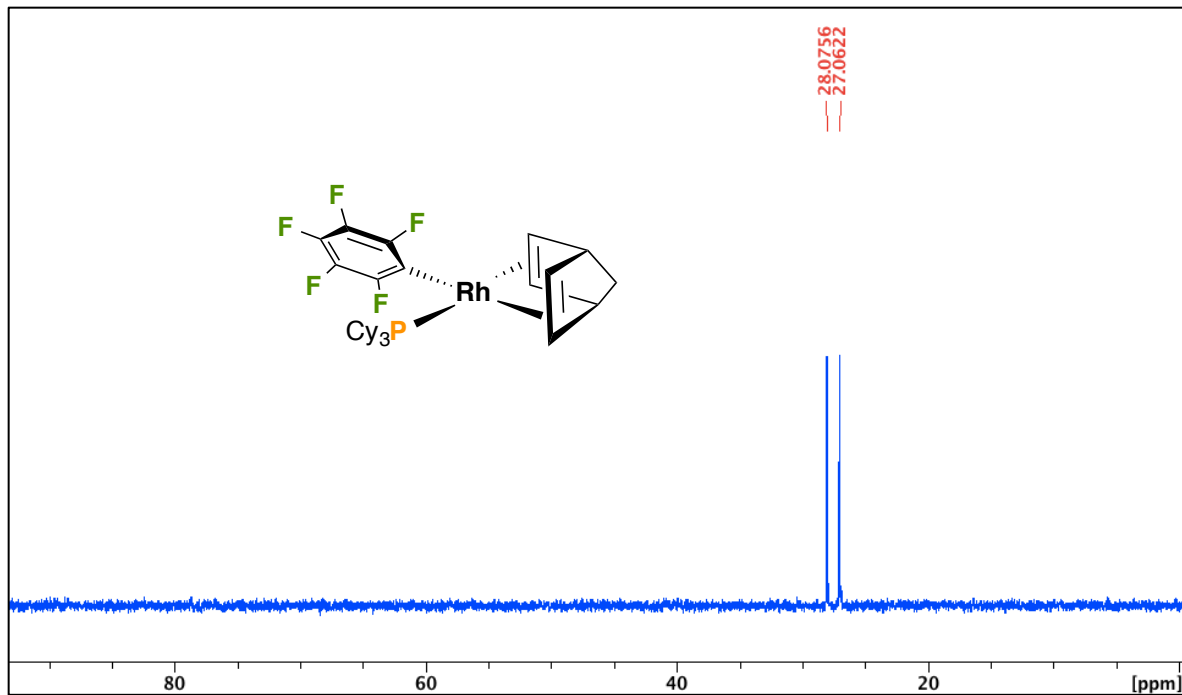


Figure S12. ${}^5\text{S}$, ${}^{13}\text{C}\{{}^1\text{H}\}$ NMR, C_6D_6 , 100 MHz, 298 K

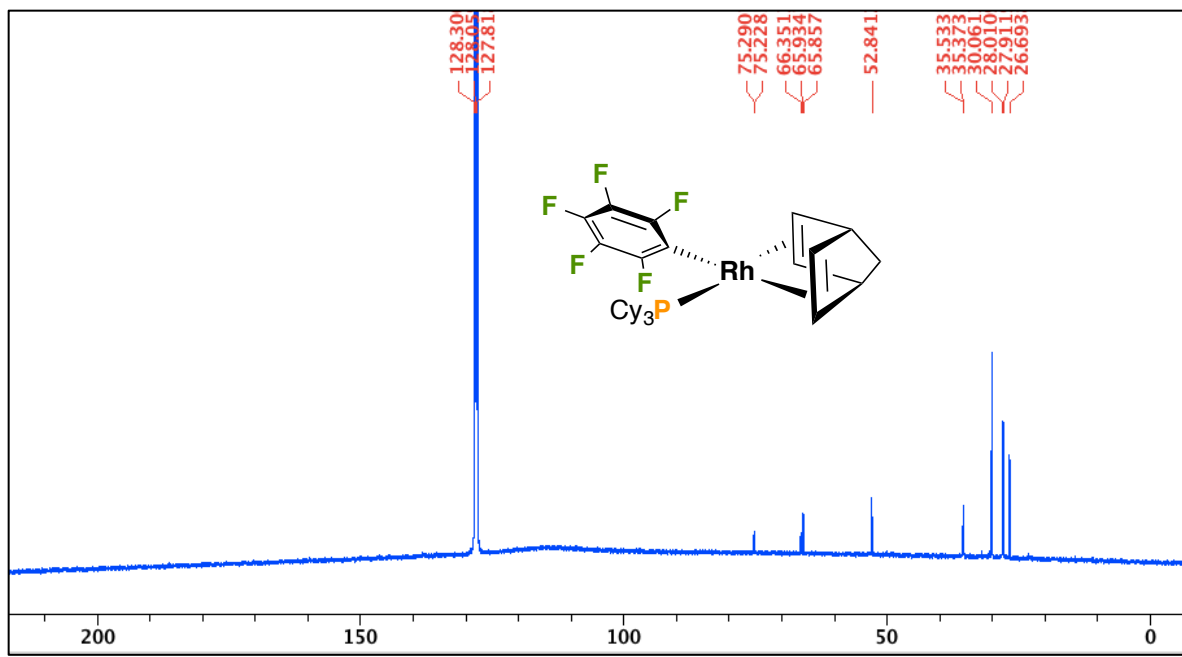


Figure S13. 6, ^1H NMR, C_6D_6 , 400 MHz, 298 K

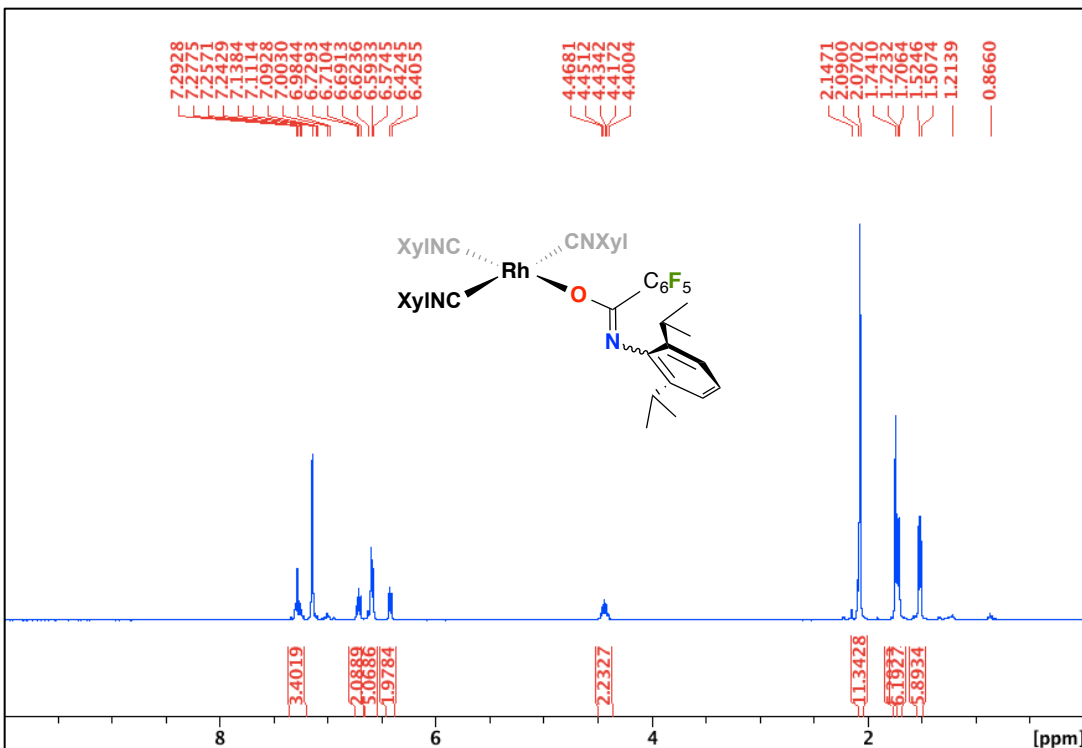


Figure S14. 6. $^{19}\text{F}\{\text{H}\}$ NMR, C_6D_6 , 377 MHz, 298 K

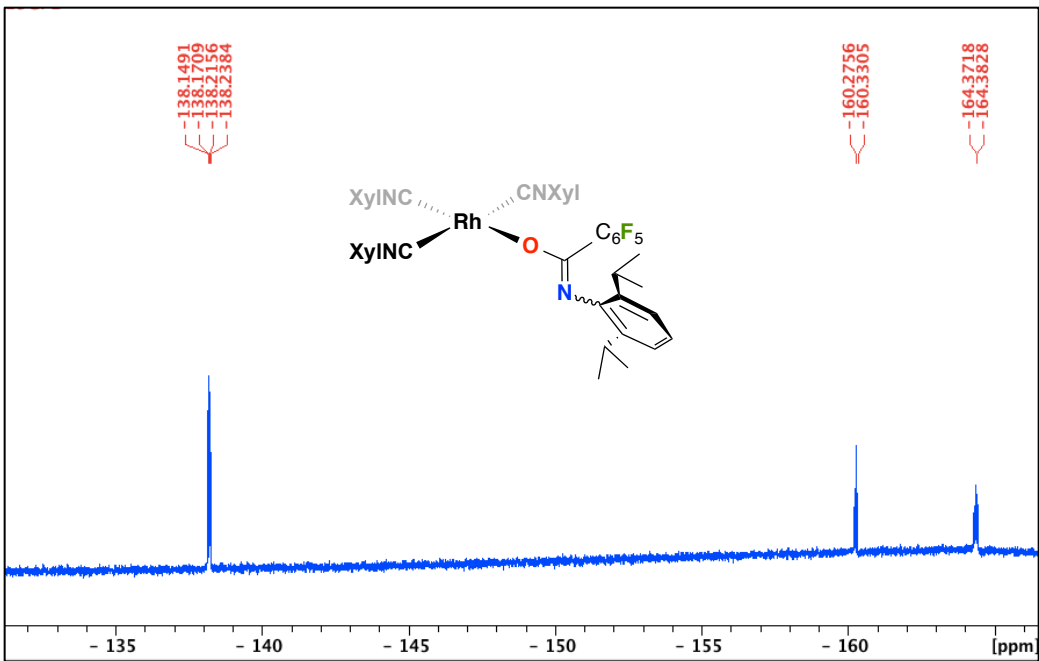


Figure S15. 6. $^{13}\text{C}\{\text{H}\}$ NMR, C_6D_6 , 100 MHz, 298 K

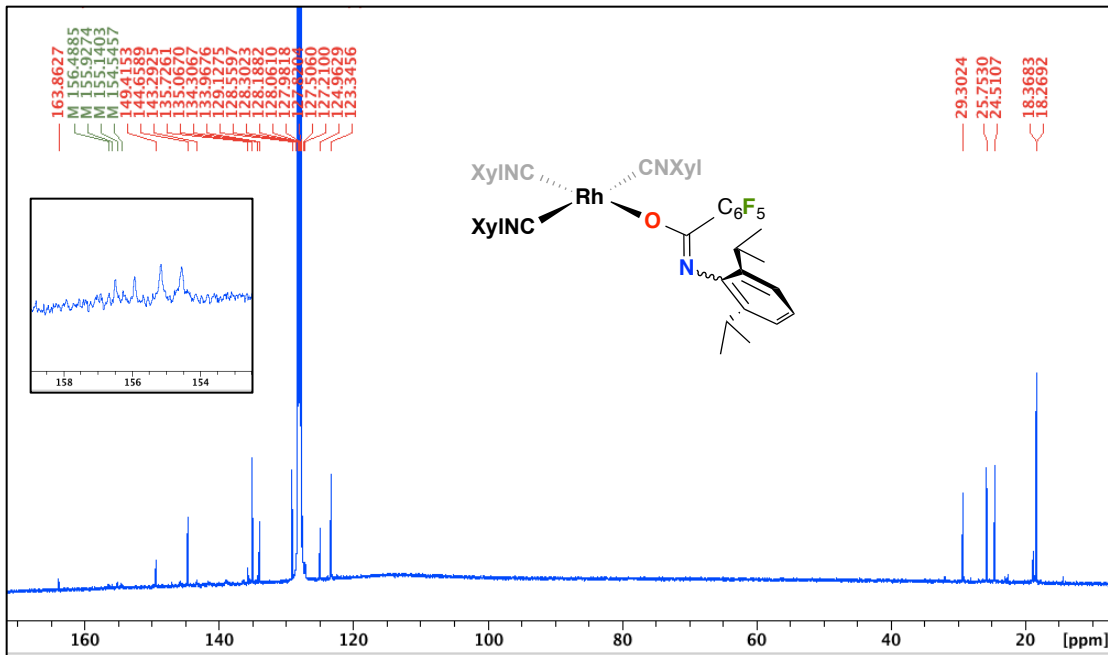


Figure S16. 6, solid-state IR (ATR) spectrum, 298 K

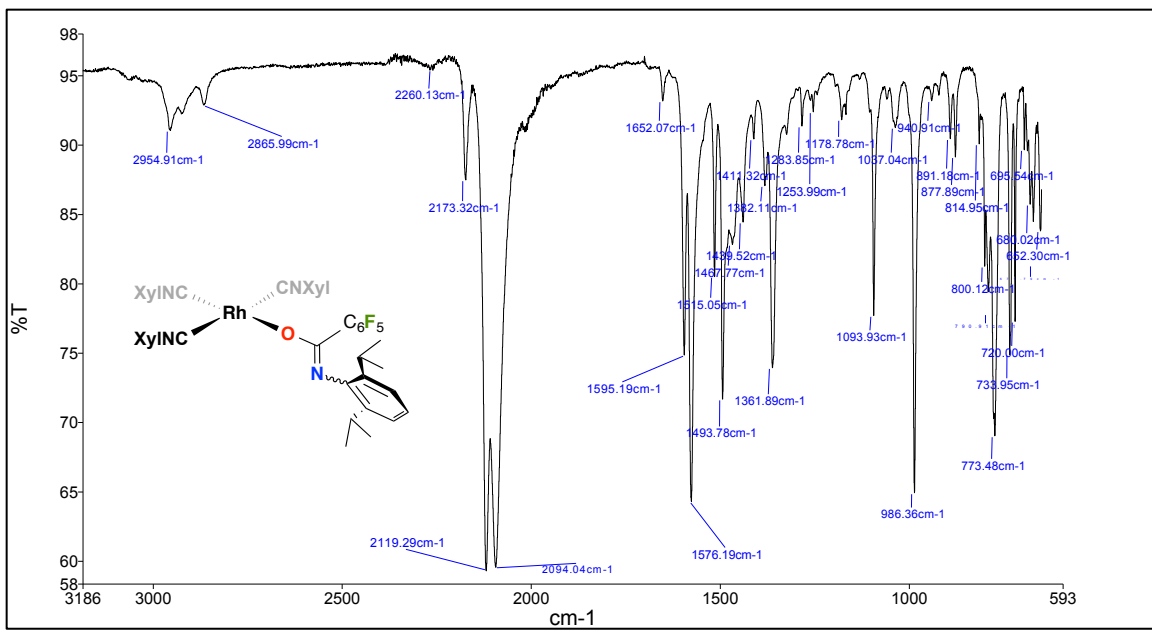


Figure S17. 7, ^1H NMR, C_6D_6 , 400 MHz, 298 K

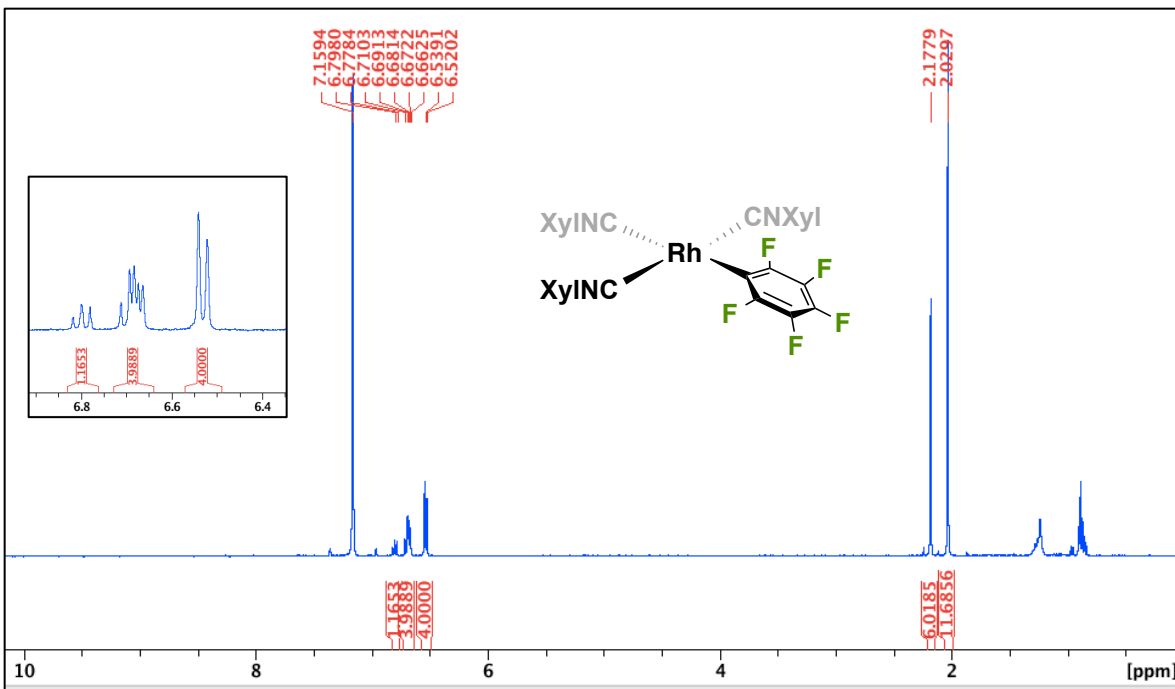


Figure S18. 7. $^{19}\text{F}\{\text{H}\}$ NMR, C_6D_6 , 377 MHz, 298 K

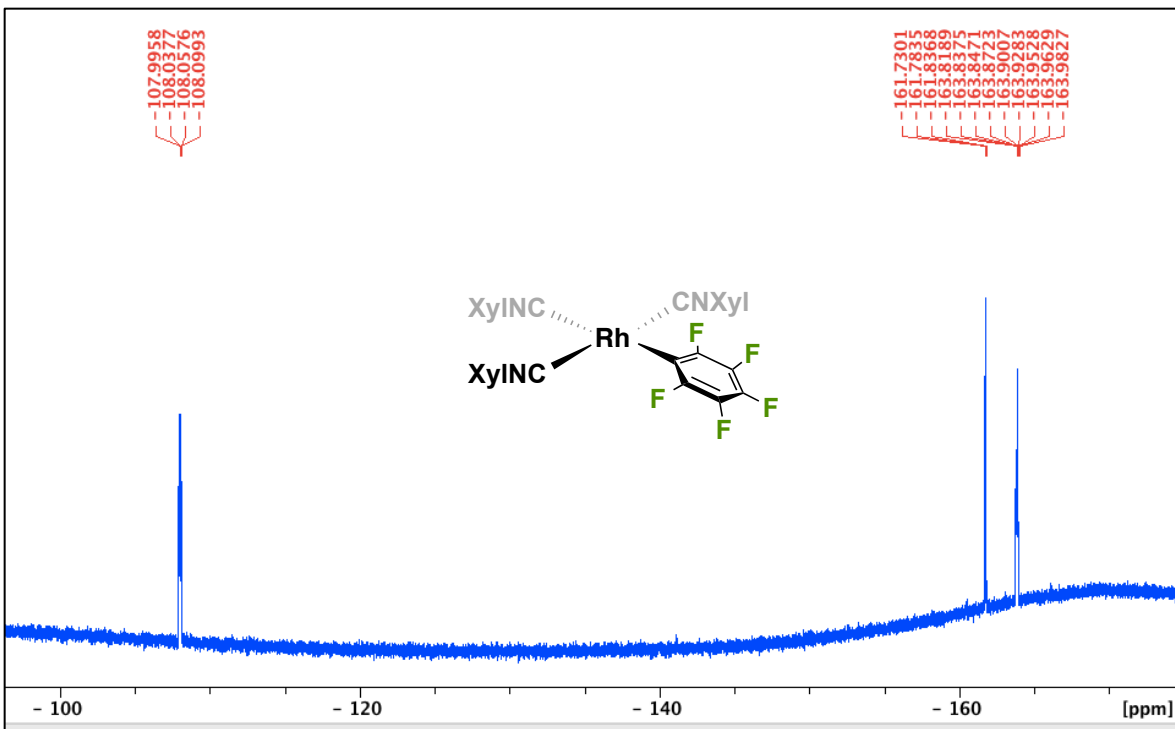


Figure S19. 7, solid-state IR (ATR) spectrum, 298 K

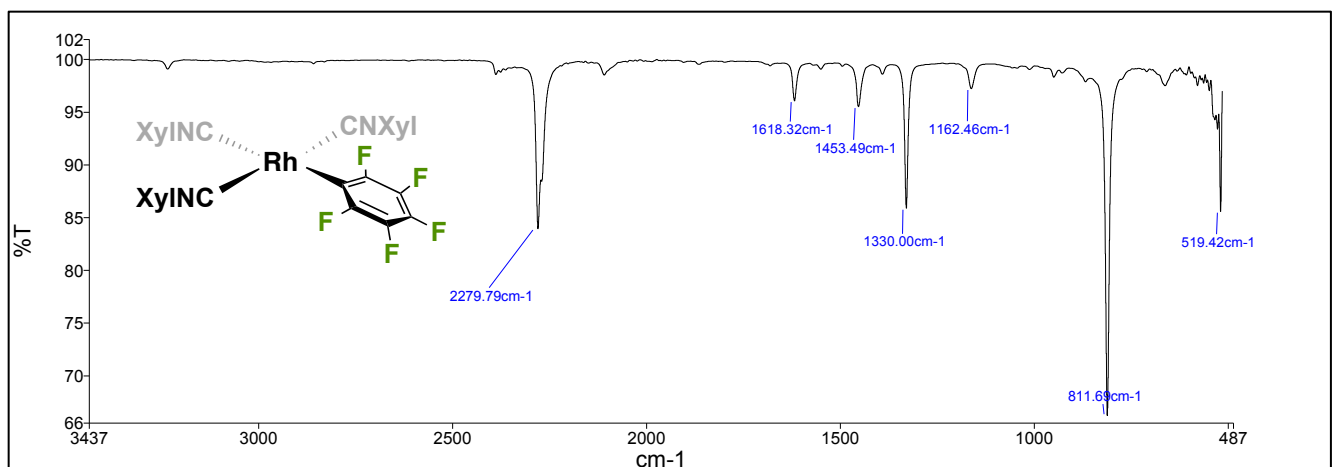


Figure S20. 8+PPh₃, ¹H NMR, C₆D₆, 400 MHz, 298 K

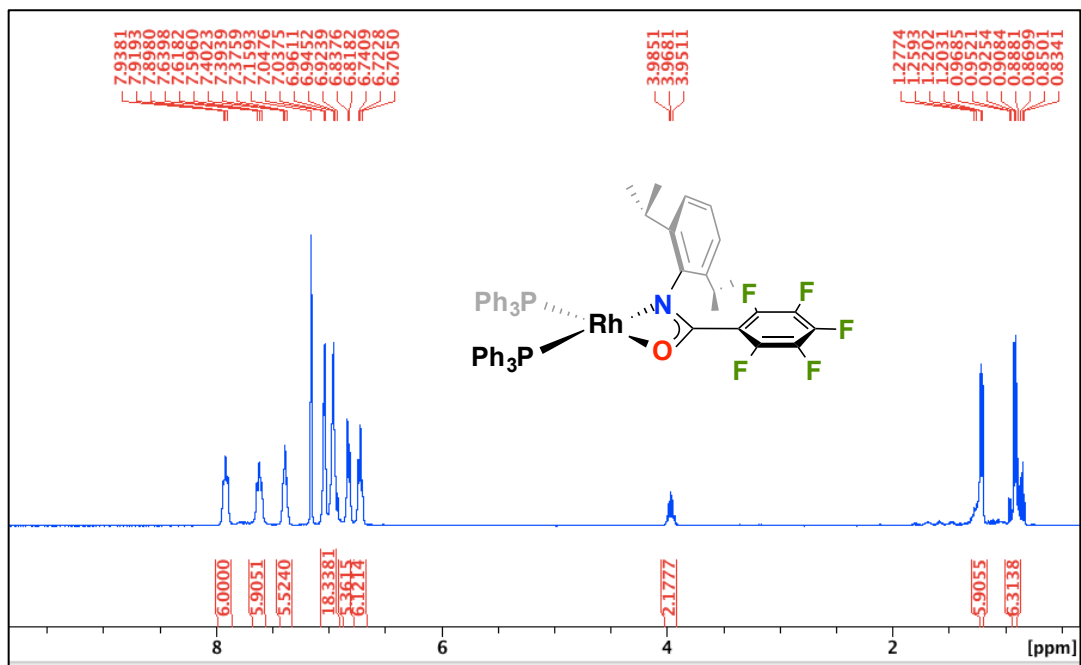


Figure S21. $\mathbf{8} + \text{PPh}_3$, ${}^{31}\text{P}\{{}^1\text{H}\}$ NMR, C_6D_6 , 162 MHz, 298 K

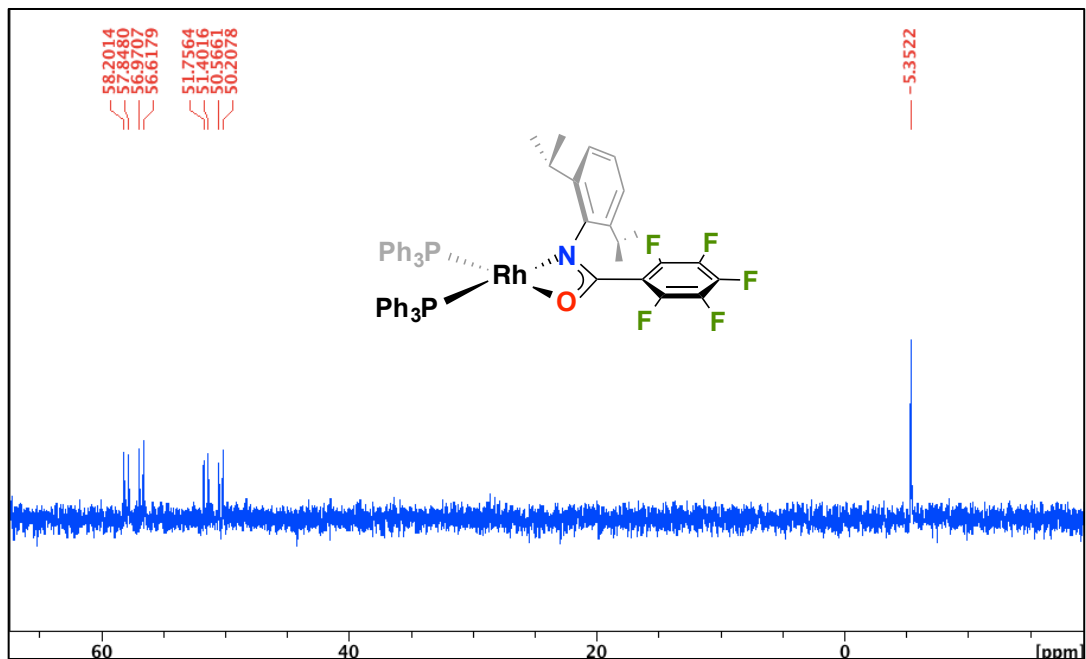


Figure S22. $\mathbf{8} + \text{PPh}_3$, ${}^{19}\text{F}\{{}^1\text{H}\}$ NMR, C_6D_6 , 377 MHz, 298 K

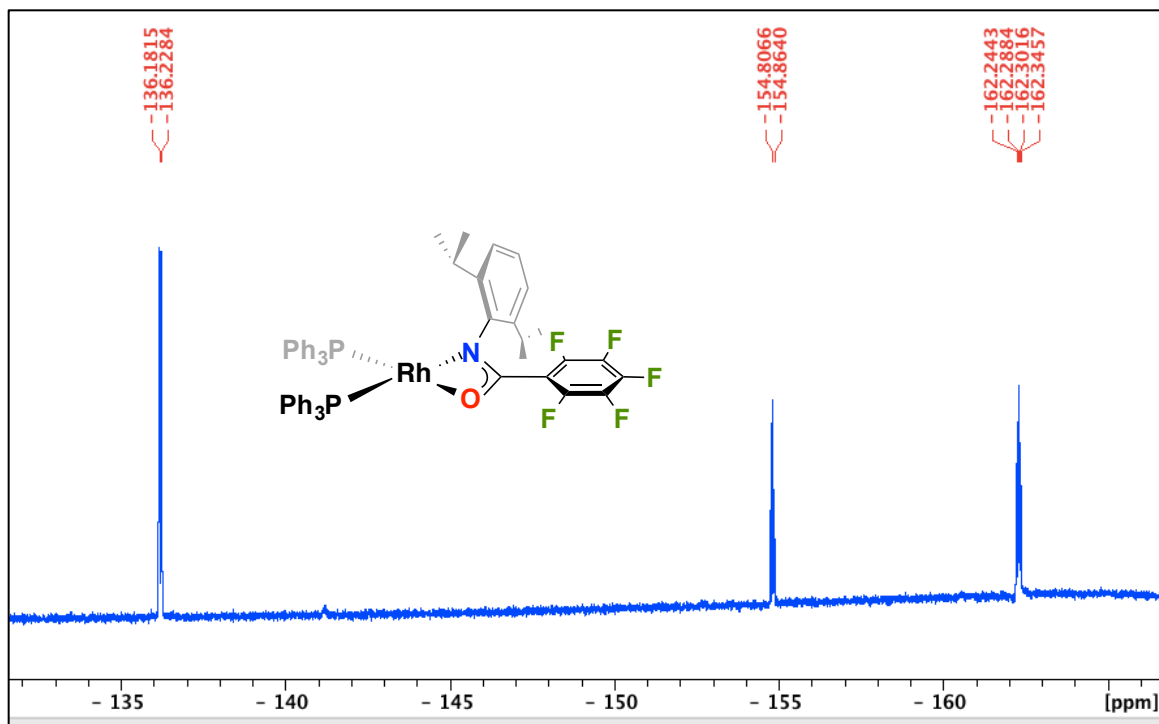


Figure S23. $\mathbf{8} + \mathbf{PPh_3}$, $^{13}\text{C}\{^1\text{H}\}$ NMR, tol- d_8 , 100 MHz, 298 K

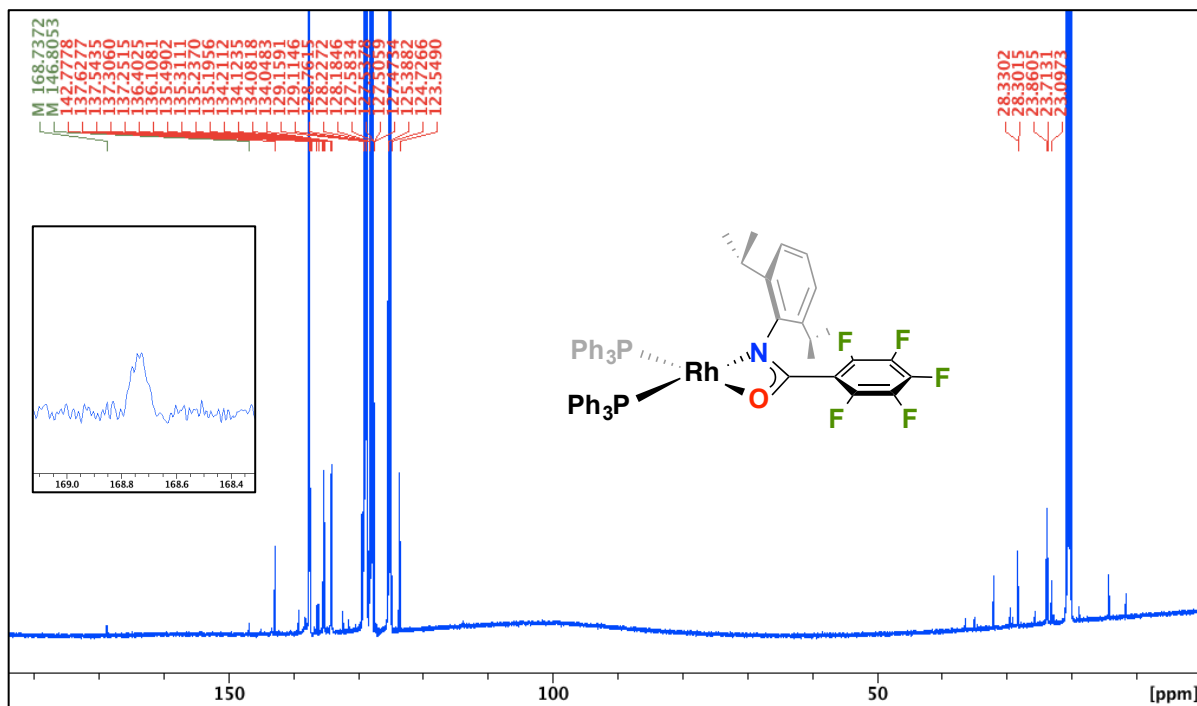


Figure S24. 8+PPh₃, VT ¹H NMR, tol-*d*₈, 400 MHz

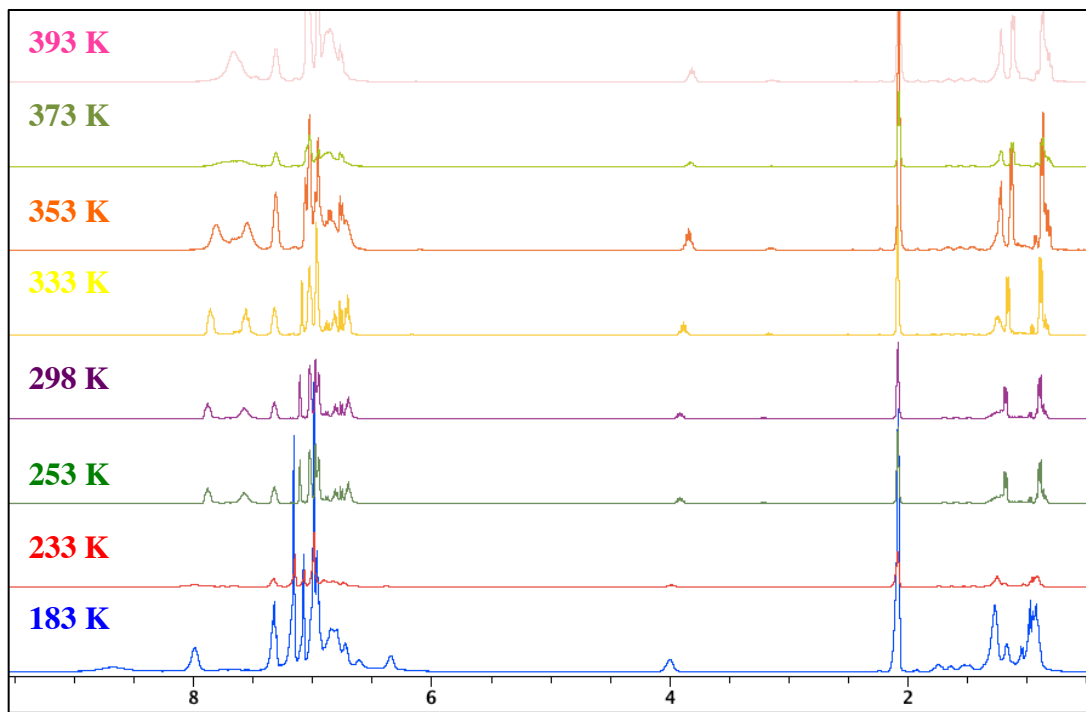


Figure S25. **8+PPh₃**, VT ³¹P{¹H} NMR, tol-d₈, 400 MHz

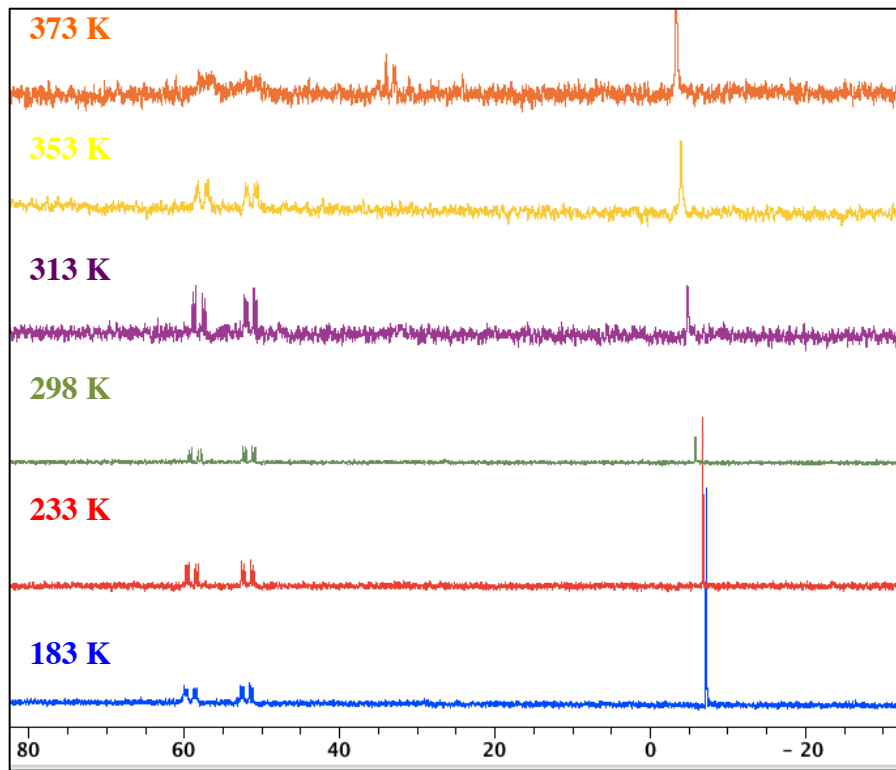


Figure S26. **8+PPh₃**, solid-state IR (ATR) spectrum, 298 K

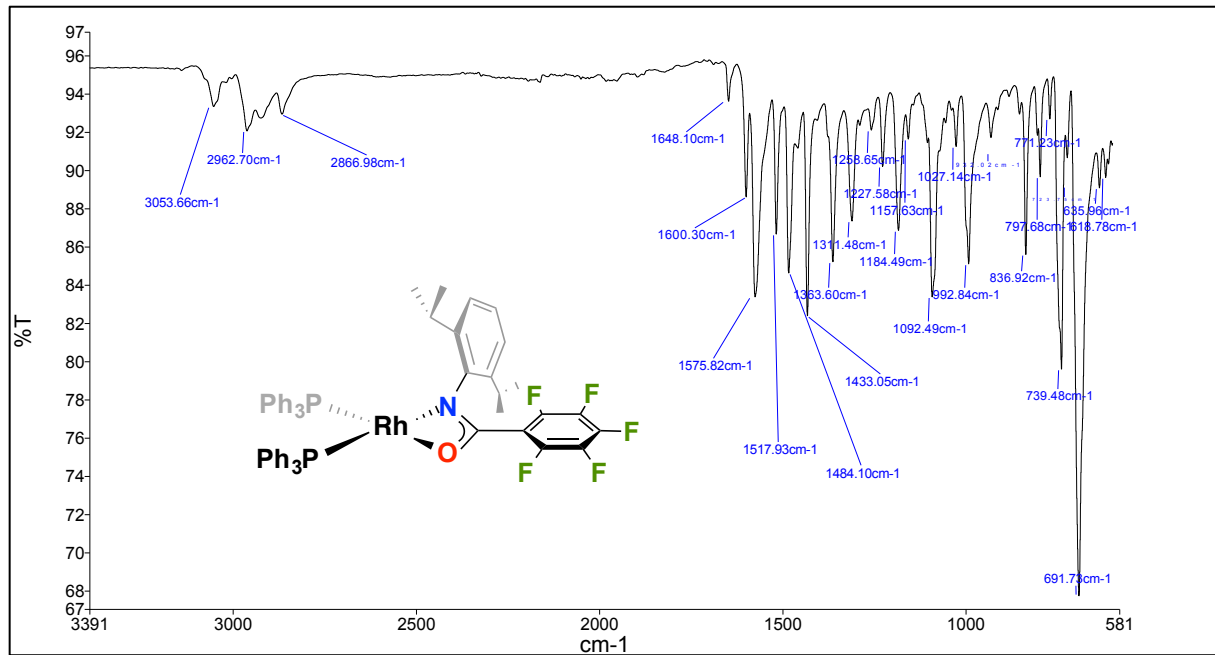


Figure S27. 10, ^1H NMR, C_6D_6 , 400 MHz, 298 K (* = trace solvent impurity (THF, Et_2O))

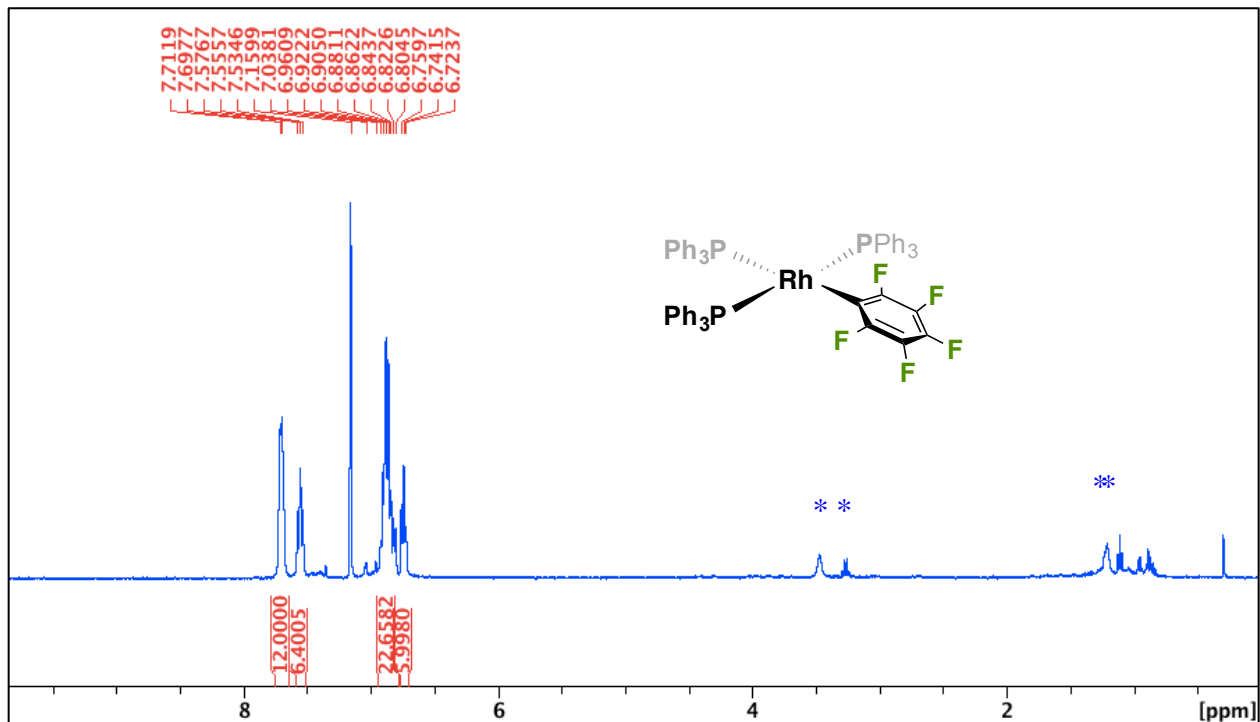


Figure S28. 10, $^{31}\text{P}\{\text{H}\}$ NMR, C_6D_6 , 162 MHz, 298 K

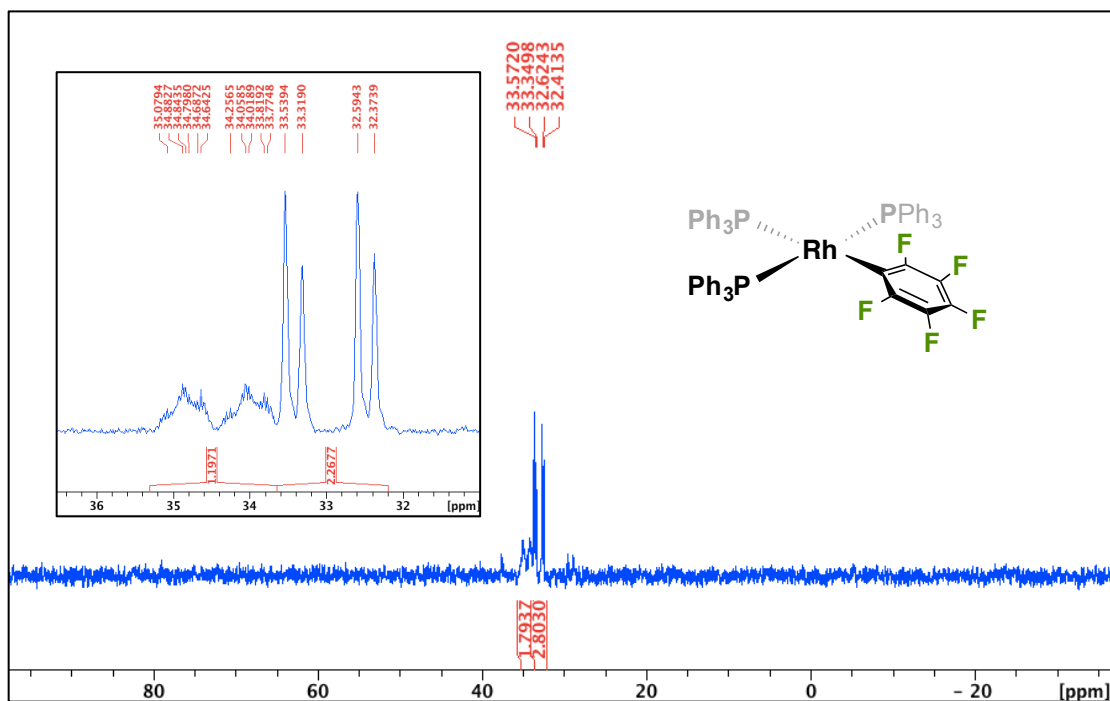


Figure S29. 10, $^{19}\text{F}\{\text{H}\}$ NMR, C_6D_6 , 377 MHz, 298 K

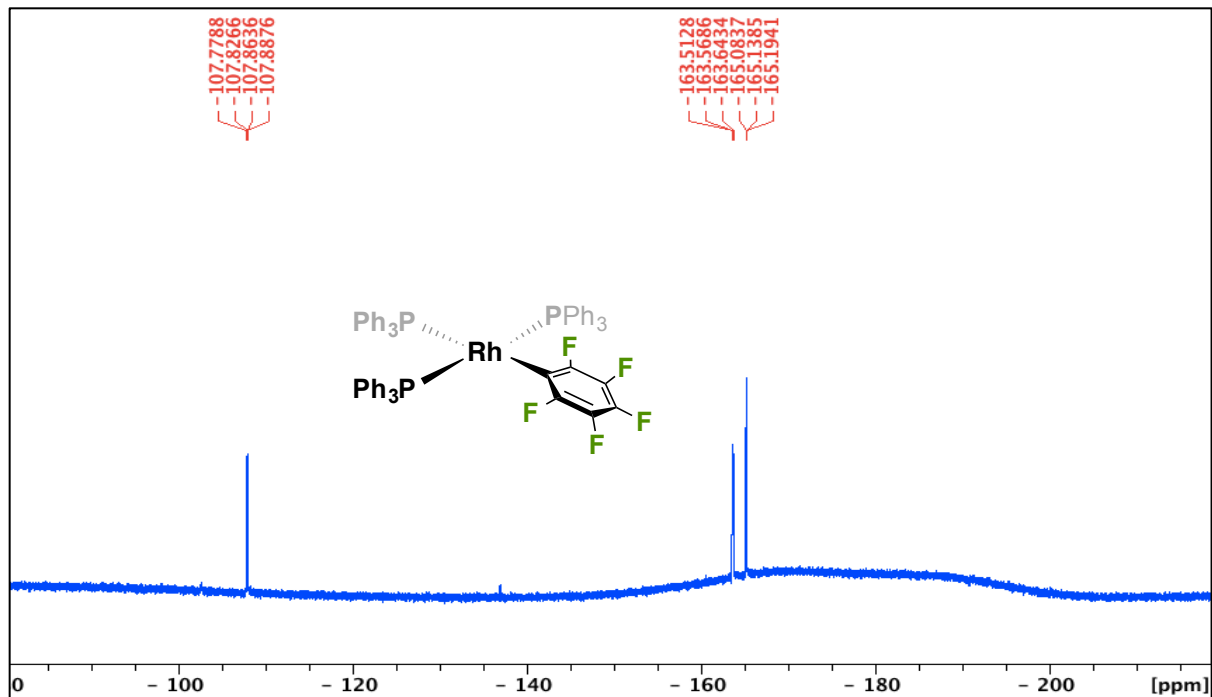


Figure S30. 10, $^{13}\text{C}\{\text{H}\}$ NMR, C_6D_6 , 100 MHz, 298 K

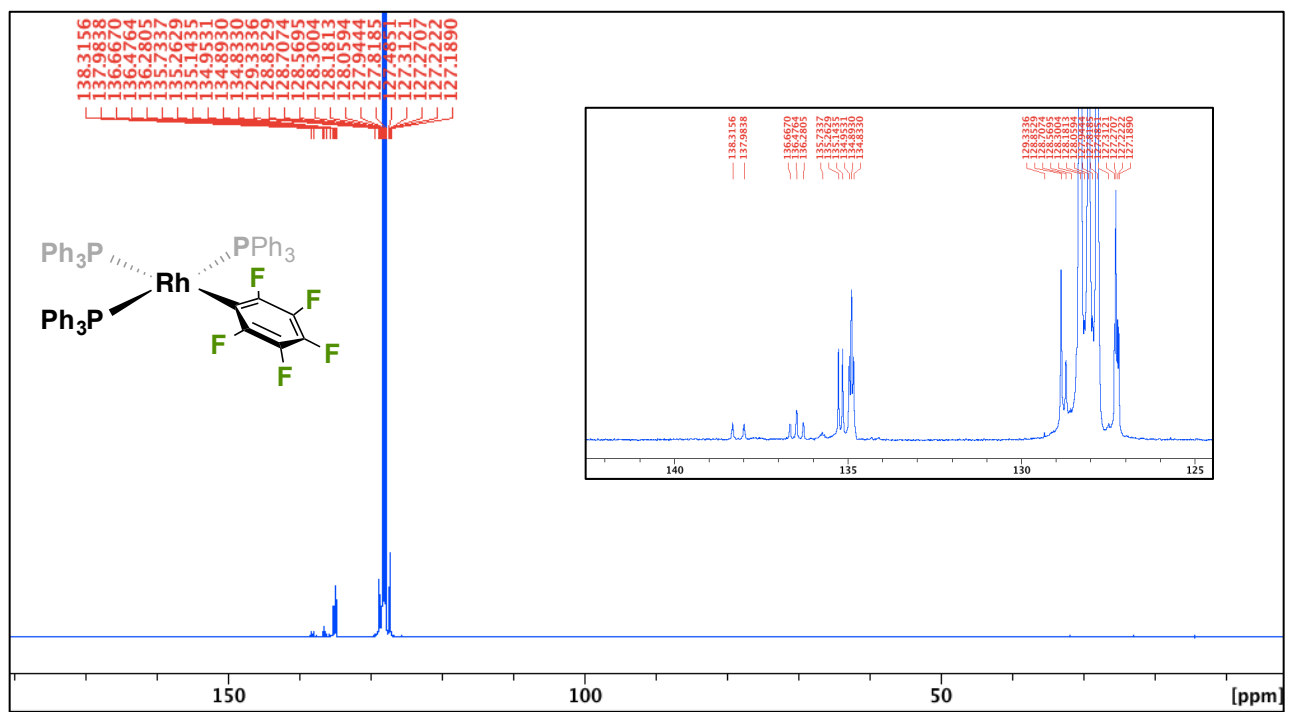


Figure S31. 2,6-diisopropylphenylisocyanate (**4**) following heating of **8+PPh₃** at 100 °C for 1 h in tol-d₈. ¹H NMR, tol-d₈, 300 MHz, 298 K

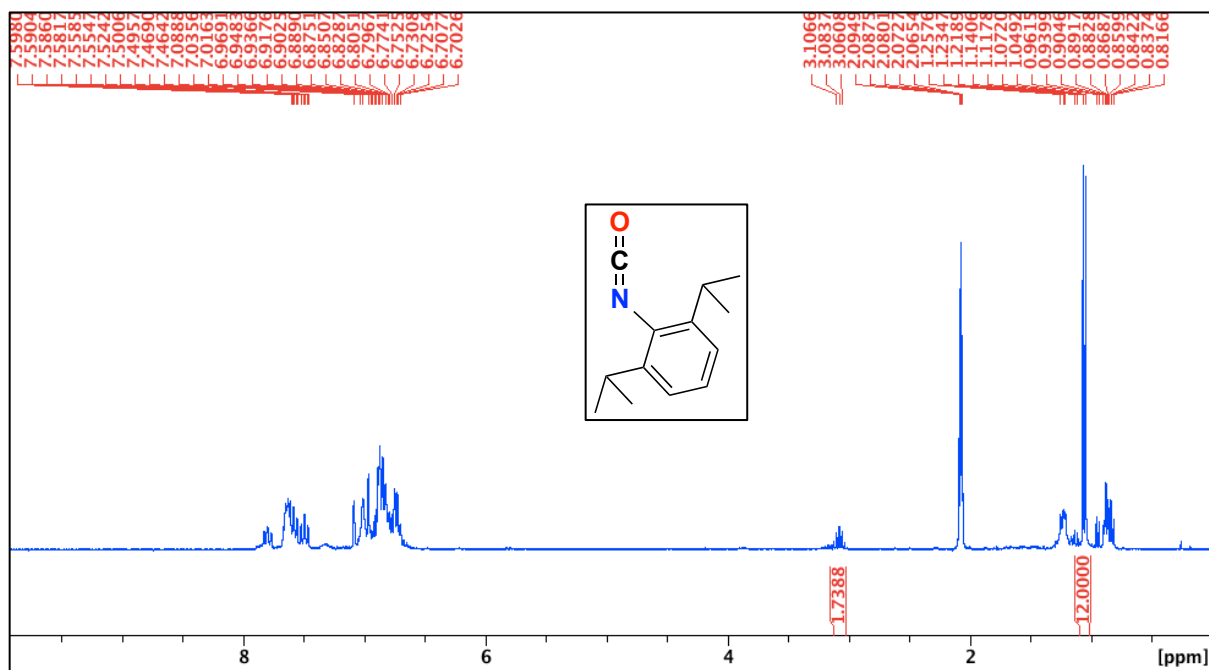


Figure S32. 2,6-diisopropylphenylisocyanate (**4**) formation following heating of **8+PPh₃** at 100 °C for 1 h in tol-d₈. ¹H NMR, tol-d₈, 400 MHz, 373 K

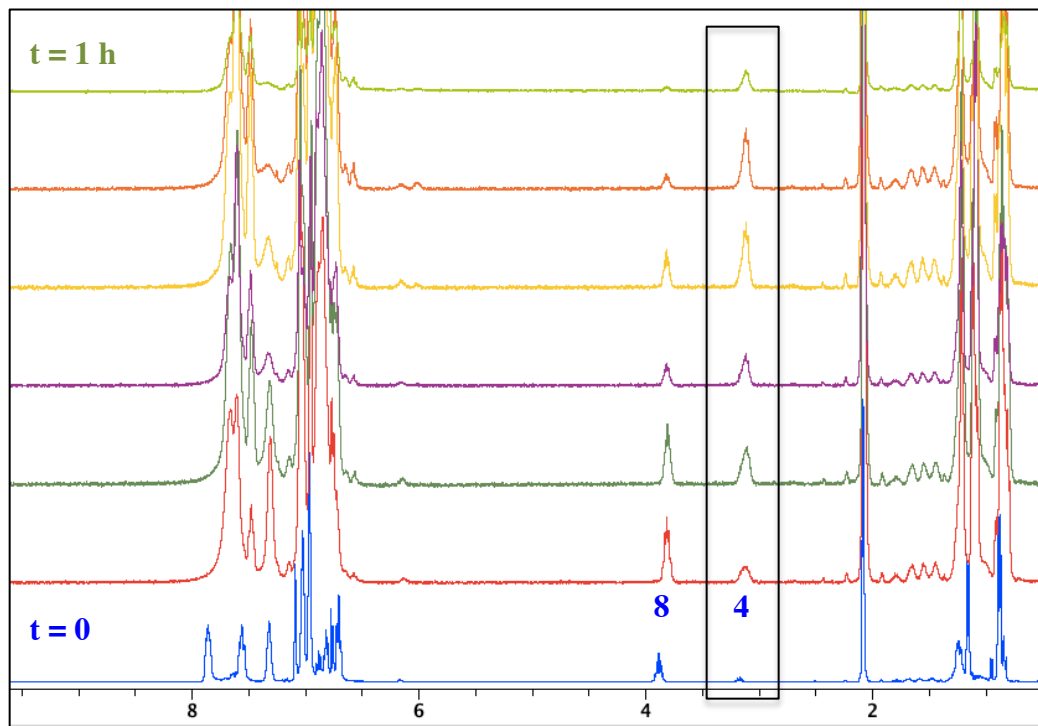


Figure S33. Rh(C₆F₅)(PPh₃)₃ formation following heating of 8+PPh₃ at 100 °C for 1 h in tol-d₈. ³¹P{¹H} NMR, tol-d₈, 162 MHz, 373 K

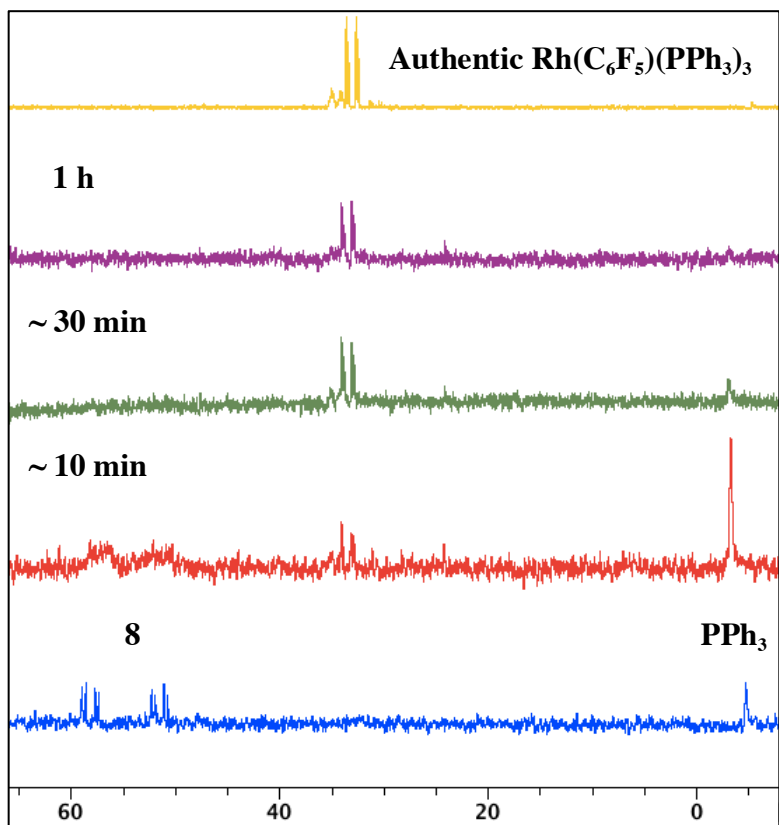


Figure S34. 2,6-diisopropylphenylisocyanate (4) in tol-d₈, IR (ATR), 298 K

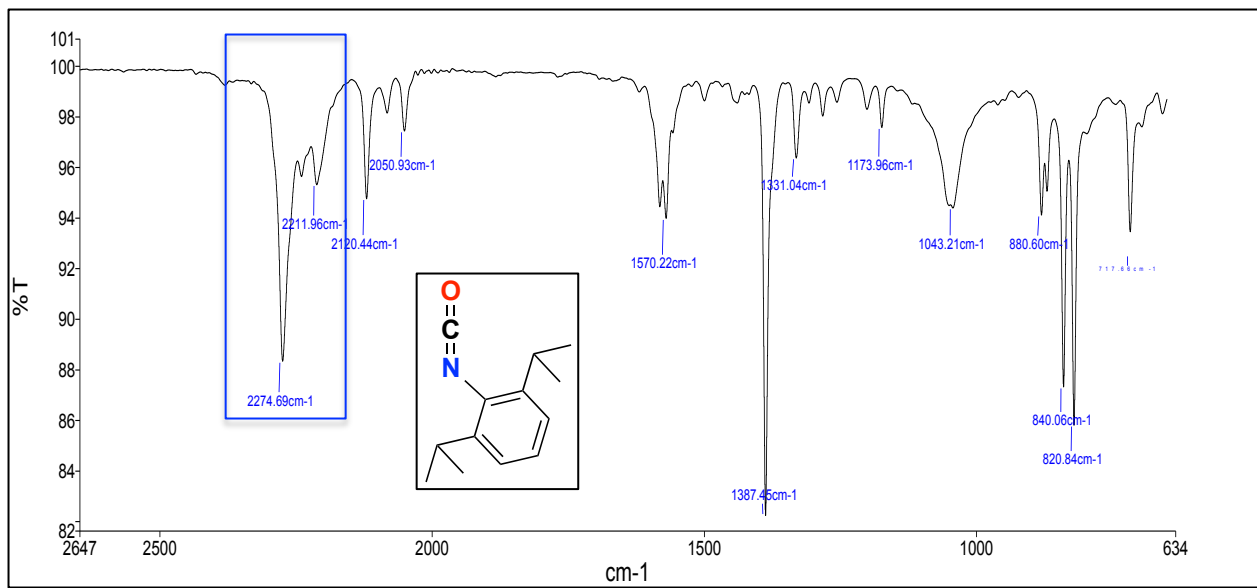


Table S1. Crystallographic data for **2** and *E/Z-3*

Compound	2	<i>E/Z-3</i>
Empirical formula	C ₅₂ H ₅₀ F ₁₀ N ₃ O ₄ Rh ₂	C _{45.5} H _{61.5} F ₅ NOPRh
Formula weight	1176.77	867.33
Temperature/K	90	90
Crystal system	Monoclinic	Triclinic
Space group	P2 ₁ /c	P-1
a/Å	18.4133(19)	9.9058(8)
b/Å	13.6493(13)	21.0289(17)
c/Å	20.839(2)	21.6355(16)
α/°	90	102.878(3)
β/°	101.855(3)	99.532(3)
γ/°	90	90.372(3)
Volume/Å ³	5125.7(9)	4328.4(6)
Z	4	4
ρ _{calc} g/cm ³	1.525	1.331
μ/mm ⁻¹	0.727	0.487
F(000)	2380.0	1818.0
Crystal size/mm ³	0.31 × 0.16 × 0.09	0.41 × 0.21 × 0.13
Radiation	MoKα (λ = 0.71073)	MoKα (λ = 0.71073)
2Θ range for data collection/°	3.59 to 60.282	2.454 to 50.802
Index ranges	-25 ≤ h ≤ 25, -19 ≤ k ≤ 19, -28 ≤ l ≤ 29	-11 ≤ h ≤ 11, -25 ≤ k ≤ 24, 0 ≤ l ≤ 26
Reflections collected	14974	15659
Independent reflections	14974 [R _{sigma} = 0.0835]	15659 [R _{sigma} = 0.0779]
Data/restraints/parameters	14974/0/613	15659/0/991
Goodness-of-fit on F ²	0.961	1.057
Final R indexes [I>=2σ (I)]	R ₁ = 0.0449, wR ₂ = 0.0824	R ₁ = 0.0528, wR ₂ = 0.1349
Final R indexes [all data]	R ₁ = 0.0780, wR ₂ = 0.0908	R ₁ = 0.0798, wR ₂ = 0.1457

Table S2. Crystallographic data for **5** and **10**

Compound	5	10
Empirical formula	C ₃₁ H ₄₁ F ₅ PRh	C _{65.94} H _{58.87} F ₅ P ₃ Rh
Formula weight	642.52	1142.12
Temperature/K	90	90
Crystal system	Monoclinic	Monoclinic
Space group	P2 ₁ /n	P2 ₁ /n
a/Å	11.6503(12)	11.1408(7)
b/Å	20.980(2)	37.184(2)
c/Å	11.7247(13)	12.9377(8)
α/°	90	90
β/°	91.257(2)	96.3810(10)
γ/°	90	90
Volume/Å ³	2865.2(5)	5326.4(6)
Z	4	4
ρ _{calc} g/cm ³	1.490	1.424
μ/mm ⁻¹	0.704	0.471
F(000)	1328.0	2358.0
Crystal size/mm ³	0.4 × 0.27 × 0.07	0.43 × 0.14 × 0.12
Radiation	Mo Kα ($\lambda = 0.71073$)	Mo Kα ($\lambda = 0.71073$)
2Θ range for data collection/°	3.882 to 61.118	3.84 to 52.12
Index ranges	-16 ≤ h ≤ 16, -29 ≤ k ≤ 29, -16 ≤ l ≤ 16	-13 ≤ h ≤ 13, -45 ≤ k ≤ 45, -15 ≤ l ≤ 15
Reflections collected	35522	49268
Independent reflections	8756 [R _{int} = 0.0326, R _{sigma} = 0.0247]	10500 [R _{int} = 0.0827, R _{sigma} = 0.0669]
Data/restraints/parameters	8756/0/343	10500/711/733
Goodness-of-fit on F ²	1.054	1.012
Final R indexes [I>=2σ (I)]	R ₁ = 0.0355, wR ₂ = 0.0891	R ₁ = 0.0414, wR ₂ = 0.0765
Final R indexes [all data]	R ₁ = 0.0400, wR ₂ = 0.0927	R ₁ = 0.0694, wR ₂ = 0.0853